

Higher-Order Non-Oscillatory Schemes in Two-Dimensional Ideal Magnetohydrodynamics

Debojyoti Ghosh* Avijit Chatterjee†

Department of Aerospace Engineering,
Indian Institute of Technology Bombay
Mumbai 400076, India

Abstract

In recent years, there has been a growing interest in the numerical solution of the MHD system, particularly the idealized system, which is obtained by neglecting dissipative effects. High-resolution schemes, which were successfully applied to the Euler equations, have been tried for the MHD equations. The non-convexity and coincidence of eigenvalues for some cases raises additional questions regarding the convergence of numerical schemes and admissibility of various non-evolutionary discontinuities. A high-resolution algorithm which uses ENO/WENO-based solution reconstruction has been implemented for the 2D MHD equations. The computation is based on the Roe scheme with the appropriate entropy fix. The solution is reconstructed via characteristic decoupling of the flux and state vectors. The code has been validated on a range of problems using Cartesian grids and some selected results are presented.

Keywords: Ideal Magnetohydrodynamics, ENO, WENO, characteristics, high-resolution schemes

Introduction

The equations of ideal magnetohydrodynamics (MHD) describe the flow of a perfectly conducting, inviscid fluid in the presence of a magnetic field [1, 2]. The dynamics of a conducting fluid can be described by extending the Navier-Stokes equations to include terms describing the momentum and energy exchange between the fluid elements and the electromagnetic field. The evolution of the electric and magnetic fields are governed by the Maxwell's equations of electromagnetics. The ideal MHD equations are obtained by a series of simplifying assumptions (like perfect conductivity, neglecting of dissipative mechanisms and displacement currents, macroscopic neutrality, etc) which are valid for a large class of plasma flows. Thus, they can be viewed as an extension of the Euler equations of gasdynamics incorporating the momentum and energy terms due to the interaction of fluid elements with the magnetic field. Along with the fluid equations, the evolution of the magnetic field is governed by the "induction equation". These equations find application in a wide range of subjects like the flow of astrophysical jets [7], flow around hypersonic vehicles [3] and controlled fusion reactions [2].

The ideal MHD equations form a non-strictly hyperbolic system where, upto six, out of the eight eigenvalues can coincide. It has also been shown that these equations are non-convex [4], thus allowing for the formation of compound waves, e.g, consisting of a rarefaction wave attached to a shock of the same family. These properties prevent the straightforward application of Godunov-type algorithms developed for the Euler equations to the MHD system. Many issues, especially the question of shock admissibility, are yet to be resolved [11]. An additional complexity for the MHD system is the necessity to ensure zero divergence of the magnetic field. Neglecting this may lead to the numerical error in computations accumulating over time and this leads to non-physical solutions, where the energy and momentum are not conserved quantities of the flow [10]. Different methods have been proposed to ensure this, including derivation of a eight-wave non-conservative formulation [6, 7] and the use of staggered grids [9].

*Graduate student (Corresponding Author), Email: ghosh@aero.iitb.ac.in, Phone: +91-9819811233

†Assoc. Professor, Email: avijit@aero.iitb.ac.in, Phone: +91-22-25767128

Following the successful application of high resolution upwind schemes to hyperbolic systems like the Euler equations of gas-dynamics and the Maxwell's equations of electromagnetics, these have also been applied to the MHD system. Brio and Wu [4] introduced an upwind differencing scheme for the 1D system which was based on a Roe-type approximate Riemann solver and demonstrated its superiority over earlier methods. The drawback of their scheme was that a Roe averaged Jacobian could not be found except in the case $\gamma = 2$. Zachary and Collela [5] applied a modification of the Engquist - Osher flux to the equations of 1D MHD. The eigenstructure of the 1D MHD system was also studied and the eigenvectors proposed by Roe and Balsara [13] have been accepted. Cargo and Gallice [12] outlined the construction of Roe matrices for the ideal MHD for the general case though their results do not show marked improvements over schemes using arithmetic averaging. The insensitivity of the computed flux to the averaged interface state was shown in [13] and thus, most schemes use arithmetic averaging to find the interface state and compute the eigenvalues and eigenvectors. Recently, the class of HLL schemes (including HLLC, HLLEM, etc) have also been applied to the 1D MHD system [8] (see references therein). Extension of these 1D schemes to multi-dimensions have not been straightforward [6, 7, 9] and methods used to ensure the solenoidal nature of the magnetic field have been employed.

The Essentially Non-Oscillatory (ENO) and Weighted Essentially Non-Oscillatory (WENO) family of schemes have been applied to the Euler equations as well as the equations of electromagnetics with excellent results. Previous attempts have been made to apply the flux-differencing form of the WENO schemes to the MHD system [14, 15] and the results are encouraging. In previous studies [18], the ENO and WENO schemes were applied to the equations of ideal 1D MHD and the performance of these high-resolution schemes were compared for the two coplanar MHD Riemann problems formulated in [4]. In the present study, the 1D algorithm has been extended to 2D. This has necessitated the use of the 8-wave formulation [6, 7] to maintain the solenoidal nature of the computed solution, thereby resulting in non-conservative governing equations. Presently, a higher-order extension of the Roe's scheme using ENO/WENO reconstruction has been implemented where the fluxes and the state vectors are reconstructed using the 2nd and 3rd order ENO and the 5th order WENO schemes via characteristic decoupling. A number of test cases have been solved for to validate the the code and these include hydrodynamic Riemann problems, oblique shock reflection problem, the rotor problem [16], the cloud-shock interaction problem [16] and the Orszag-Tang vortex problem [9]. Representative results have been presented here.

Governing Equation

The ideal MHD equations are obtained by considering the flow of an inviscid, perfectly conducting fluid in the presence of a magnetic field and can be expressed as [1, 2]:

$$\rho_t + \nabla \cdot (\rho \mathbf{u}) = 0 \quad (1)$$

$$(\rho \mathbf{u})_t + \nabla \cdot (\rho \mathbf{u} \mathbf{u} + \gamma P^* \mathcal{I} - \frac{\mathbf{B} \mathbf{B}}{\mu}) = \mathbf{0} \quad (2)$$

$$\mathbf{B}_t + \nabla \cdot (\mathbf{u} \mathbf{B} - \mathbf{B} \mathbf{u}) = \mathbf{0} \quad (3)$$

$$E_t + \nabla \cdot [(E + P^*) \mathbf{u} - \frac{1}{\mu} (\mathbf{u} \cdot \mathbf{B}) \mathbf{B}] = 0 \quad (4)$$

where $P^* = p + \mathbf{B} \cdot \mathbf{B} / 2\mu$ is the full pressure (defined as the sum of gas pressure and the magnetic pressure) and $E = \rho \mathbf{u} \cdot \mathbf{u} / 2 + p / (\gamma - 1) + \mathbf{B} \cdot \mathbf{B} / 2\mu$ is the total energy of the system. Additionally, the divergence free condition $\nabla \cdot \mathbf{B} = 0$ needs to be satisfied. Theoretically, if the initial conditions satisfy this constraint, then the solution at all time satisfies it. However, in numerical computations, small errors can arise which causes non-zero divergence of the magnetic field. These considerations are important while solving multi-dimensional problems.

The equations of 2D ideal MHD can be expressed in the conservative form as [9]:

$$\frac{\partial \mathbf{u}}{\partial t} + \nabla \cdot \mathbf{F} = 0 \quad (5)$$

where the flux is $\mathbf{F} = \mathbf{f}\hat{\mathbf{i}} + \mathbf{g}\hat{\mathbf{j}}$, $\mathbf{u} = [\rho \ \rho u \ \rho v \ \rho w \ B_x \ B_y \ B_z \ E]^T$ and

$$\mathbf{f}(\mathbf{u}) = \begin{bmatrix} \rho u \\ \rho u^2 + P^* - B_x^2 \\ \rho uv - B_y B_x \\ \rho uw - B_z B_x \\ 0 \\ u B_y - v B_x \\ u B_z - w B_x \\ (E + P^*)u - B_x \mathbf{u} \cdot \mathbf{B} \end{bmatrix}, \quad \mathbf{g}(\mathbf{u}) = \begin{bmatrix} \rho v \\ \rho uv - B_x B_y \\ \rho v^2 + P^* - B_y^2 \\ \rho vw - B_z B_y \\ v B_x - u B_y \\ 0 \\ v B_z - w B_y \\ (E + P^*)v - B_y \mathbf{u} \cdot \mathbf{B} \end{bmatrix} \quad (6)$$

The above equations are non-strictly hyperbolic and have non-convex flux functions. Additionally, while solving these equations numerically, it is imperative to ensure the solenoidal nature of the computed magnetic field. While in 1D, this condition reduces to $B_x = \text{constant}$ and is satisfied by leaving out B_x from the evolution equations; it becomes more complicated in 2D and 3D. The magnetic field is required to satisfy:

$$\nabla \cdot \mathbf{B} = 0 \Rightarrow \oint \mathbf{B} \cdot \hat{\mathbf{n}} dS = 0 \Rightarrow \sum_{\text{faces}} \mathbf{B} \cdot \hat{\mathbf{n}} \delta S = 0 \quad (7)$$

A number of methods have been developed to enforce this condition in numerical computations as discussed in [9]. In the present study, the 8-wave formulation developed in [6, 7] has been used.

The 8-wave Formulation

The 8-wave formulation is derived from adding a source term proportional to the divergence of \mathbf{B} to the governing equation (5). This equation can be derived from the basic equations of magnetohydrodynamics by *not* assuming that the divergence of \mathbf{B} is zero and retaining terms containing $\nabla \cdot \mathbf{B} = \mathbf{0}$ [7]. The aim is to obtain a symmetrizable form of the MHD equations. Equation (5) admits a zero eigenvalue which is non-physical in nature. The modified 8-wave formulation replaces this eigenvalue with u_n (the fluid velocity normal to the face) and thus all eigenvalues are symmetric about the fluid velocity. The modified governing equation is as follows:

$$\frac{\partial \mathbf{u}}{\partial t} + \nabla \cdot \mathbf{F} = \mathbf{S} \quad (8)$$

where $\mathbf{S} = -(\nabla \cdot \mathbf{B})[0 \ \mathbf{B} \ \mathbf{u} \ \mathbf{u} \cdot \mathbf{B}]^T$. The effect of the source term on the divergence of \mathbf{B} can be seen by taking the divergence of all terms of the induction equation (3). Without the source term, this results in the constraint $\nabla \cdot \mathbf{B} = \mathbf{0}$. If the initial conditions satisfy this condition, the computed solution should ideally satisfy it, assuming no errors in computations. However with the source term included, one obtains

$$\frac{\partial \rho \phi}{\partial t} + \nabla \cdot (\rho \mathbf{u} \phi) = 0 \quad (9)$$

where $\phi = \nabla \cdot \mathbf{B} / \rho$. This describes the equation of the quantity ϕ which is being passively convected with the fluid. For the solution, ϕ is constant for all streak-lines and since the initial and boundary conditions satisfy the zero divergence condition, the solution should also have zero divergence. Another way to interpret the effect of adding a source term is to observe that due to the convection equation, any finite value that the divergence of \mathbf{B} may develop as the solution progresses will get convected away. However, it should be noted that the modified equations are no longer strictly conservative in nature. Ideally, when the divergence is zero, the modified and original equations are identical and thus, conservative. In numerical computations, the divergence will never be strictly zero and will have some value of the order of round-off errors. This will lead to slight errors in meeting shock jump conditions. It is expected that the effect on the solution will be negligible.

Eigenstructure

The 8-wave formulation admits eight eigenvalues. For an arbitrary face with normal $\hat{\mathbf{n}}$, the eigenvalues are as follows:

- $\lambda_e = u_n$ - entropy wave
- $\lambda_d = u_n$ - “divergence” wave
- $\lambda_s = u_n \pm c_s$ - left and right running slow waves
- $\lambda_a = u_n \pm c_a$ - left and right running Alfvén waves
- $\lambda_f = u_n \pm c_f$ - left and right running fast waves

where the wavespeeds are given by

$$c_a = B_n / \sqrt{\rho} \quad (10)$$

$$c_{f,s}^2 = \frac{1}{2} \left[\frac{\gamma p + \mathbf{B} \cdot \mathbf{B}}{\rho} \pm \sqrt{\left(\frac{\gamma p + \mathbf{B} \cdot \mathbf{B}}{\rho} \right)^2 - \frac{4\gamma p B_n^2}{\rho^2}} \right] \quad (11)$$

and the subscript n denoted quantities normal to the interface. The eigenvectors for this modified system, as derived from the primitive variables ($\mathbf{w} = [\rho \ u \ v \ w \ B_x \ B_y \ B_z \ p]^T$), have been derived in [7] for the special case of the interface being normal to the x -axis. In the present study, the eigenvectors, in terms of the conserved variables, have been derived appropriately multiplying the eigenvectors in primitive form by the Jacobians of transformation relating conserved and primitive variables. Additionally, using the rotation matrices for transformation of the velocity and magnetic fields from Cartesian coordinates to face-normal and tangential coordinates and vice versa, the eigenvectors were derived for an arbitrary face.

Numerical Scheme

The governing equation, discretized in space is given as:

$$\frac{d\mathbf{u}_{ij}}{dt} V_{ij} + \sum_{faces} \mathbf{F} \cdot \hat{\mathbf{n}} dS = \mathbf{S}_{ij} V_{ij} \Rightarrow \frac{d\mathbf{u}_{ij}}{dt} = \mathbf{Res}(i, j) \quad (12)$$

where the residual is given by (for a quadrilateral cell)

$$\mathbf{Res}(i, j) = \frac{-1}{V_{ij}} \left[\sum_{l=1}^4 \mathbf{F} \cdot \hat{\mathbf{n}}_l dS_l + \mathbf{s}_{ij} \sum_{l=1}^4 \mathbf{B} \cdot \hat{\mathbf{n}}_l dS_l \right] \quad (13)$$

where $\mathbf{s} = [0 \ \mathbf{B} \ \mathbf{u} \ \mathbf{u} \cdot \mathbf{B}]^T$. The semi-discrete ODE, as given by equation (12) is marched in time using the multi-stage Runge-Kutta (RK) algorithm. The 1st order, 2nd and 3rd order TVD RK and 4th order RK time stepping has been implemented and used in the present study. For the computation of the divergence term, the term \mathbf{s}_{ij} is computed using the values at the cell center. The magnetic flux through the faces ($\mathbf{B} \cdot \hat{\mathbf{n}}_l dS_l$) are computed by taking the arithmetic average of the magnetic field at the cells on either side of the interface.

Currently, a high-resolution solver using ENO/WENO reconstruction based on the Roe’s scheme has been implemented to compute the flux at the interface. A similar effort has been made in [7] which uses a weighted least-squares based reconstruction. The basic Roe’s scheme is given by [7]:

$$\mathbf{F} \cdot \hat{\mathbf{n}}(\mathbf{u}_L, \mathbf{u}_R) = \frac{1}{2} [(\mathbf{F} \cdot \hat{\mathbf{n}}(\mathbf{u}_L) + \mathbf{F} \cdot \hat{\mathbf{n}}(\mathbf{u}_R))] - \sum_{k=1}^8 \mathbf{L}_k(\mathbf{u}_R - \mathbf{u}_L) |\lambda_k| \mathbf{R}_k \quad (14)$$

To prevent the formation of expansion shocks, the Harten’s entropy fix [7] has been implemented. The fluxes and the state vectors are reconstructed using 2nd & 3rd order ENO and 5th order WENO schemes via characteristic decoupling.

Results and Discussions

The code is validated for test cases which have become benchmark problems for 2D MHD. The test cases reported here are the Orszag-Tang vortex problem [9, 14, 16, 17], the cloud-shock interaction [16] and the fast rotor problem [8, 16, 17]. Unless mentioned otherwise, the domain in all problems as been taken to be a square of unit length. Aside for the problems reported here, the code has also been tested on some hydrodynamic problems, since in the absence of a magnetic field, the MHD equations reduce to the Euler's equations. These test cases include the 2D Riemann problems as well as the oblique shock reflection problem.

Orszag-Tang Vortex Problem

The evolution of the Orszag-Tang vortex system has been considered in this problem. It was proposed as a simple model to study significant features of supersonic MHD turbulence and tests the code's robustness at handling the formation of shocks and shock-shock interactions. The initial data consists of a superimposition of sinusoidal velocity and magnetic fields and the flow quickly transforms to a very complex structure with multiple interacting shocks. This test problem has become a benchmark for 2D codes and has been solved for in [9, 14, 16, 17] with slightly varying initial conditions (which are all topologically similar). In the present study, the initial conditions ($\mathbf{w} = [\rho, u, v, w, B_x, B_y, B_z, p]^T$) are as follows:

$$\mathbf{w}_{initial} = [1.0, -\sin(2\pi y), \sin(2\pi x), 0, -\sin(2\pi y)/\gamma, \sin(4\pi x)/\gamma, 0, 1/\gamma]^T \quad (15)$$

with $\gamma = 1.67$. The boundary conditions are all periodic. The solution at time $t = 0.5$ was computed using a 200×200 grid. The computations were done using 1st order Roe (with 1st order time stepping), 2nd & 3rd order ENO (with 2nd order TVD RK time stepping) and 5th order WENO (with 3rd order TVD RK time stepping). Figure (1) shows the density contours obtained by using the 5th order WENO reconstructions compared with the results presented in [9]. Both these results were obtained using a 200×200 grid. A good agreement is seen with the between our results and those in [9]

Rotor Problem

The evolution of a dense, rotating fluid in an ambient, stationary fluid of lesser density is studied in this problem [8, 16, 17]. The initial conditions are identical to those specified in [16] as "Rotor problem 1". There is a disk of dense rotating fluid with $\rho = 10$, $u = -v_0(y - 0.5)/r_0$ and $v = v_0(x - 0.5)/r_0$ with a radius $r_0 = 0.1$ and $v_0 = 2$. The ambient fluid is at rest with $\rho = 1$ for $r > r_1 = 0.115$ ($r = \sqrt{(x - 0.5)^2 + (y - 0.5)^2}$). For the fluid in between ($r_0 < r < r_1$), linear density and angular speed profiles are provided with $\rho = 1 + 9f$, $u = -fv_0(y - 0.5)/r$, $v = fv_0(x - 0.5)/r$ where $f = (r_1 - r)/(r_1 - r_0)$. An uniform pressure and magnetic field exist throughout the domain ($p = 1$, $B_x = 5/\sqrt{4\pi}$) with $\gamma = 1.67$. Out-of-plane components of velocity and magnetic fields are zero. All boundaries were outgoing. The solution is obtained for a time level of 0.15. Figure (2) shows the pressure contours obtained using 3rd order ENO schemes with 2nd order time stepping on a 100×100 grid and that obtained in [16] using a constrained transport/central difference based scheme on a 400×400 grid. These computed results show a good agreement with the results in [16]. The same problem, solved in [8, 17] has slightly different initial conditions. The results are qualitatively similar.

Cloud Shock Interaction

This problem studies the interaction of a high density cloud, moving at supersonic speeds (approximately 8.7 Mach), and a stationary shock [16]. The initial conditions consist of a stationary discontinuity which is a fast shock combined with a rotational discontinuity in B_z . The left and right states are given by:

$$\mathbf{w}_L = [3.87 \ 0 \ 0 \ 0 \ 0 \ 2.18 \ -2.18 \ 167.35], \quad \mathbf{w}_R = [1 \ -11.25 \ 0 \ 0 \ 0 \ 0.56 \ 0.56 \ 1] \quad (16)$$

with $\gamma = 1.67$. The discontinuity lies at $x = 0.6$. Superimposed on these initial conditions is a high density circular cloud with $\rho = 10$, $p = 1.0$ centered at $x = 0.8$, $y = 0.5$ with a radius 0.15, moving leftwards at the same velocity as the ambient gas. The right boundary is a supersonic inflow boundary

with the conditions specified as \mathbf{w}_R while all other boundaries are outgoing. Figure (3) shows the density contours and magnetic field lines obtained from the 2nd order ENO scheme on a 200×200 grid. The computed results are compared with those obtained by [16]. Figure (4) shows the results obtained in [16] using a constrained transport/central difference type scheme on a 400×400 grid. A logarithmic gray-scale plot (white - minimum, black - maximum) of density and the magnetic field lines in the x - y plane are shown respectively. The solution has been obtained at a time level of 0.06. A good agreement is seen between the computed results and Toth's results although the resolution of latter is better (especially ahead (leftwards) of the high density cloud) due to a finer grid.

Conclusions

In the present study, a higher-order algorithm using the ENO/ WENO reconstruction based on the Roe scheme has been implemented for the 2D equations. The 2nd & 3rd order ENO and 5th order WENO spatial reconstruction and 2nd & 3rd order TVD Runge-Kutta and 4th order Runge-Kutta time-stepping has been implemented, apart from the basic 1st order scheme. Presently, the code has been validated for a number of benchmark problems involving Cartesian grids. Once the code has been validated on body-fitted grids and its performance evaluated for all kinds of boundary conditions, it is intended to carry out blunt body computations, whose results are likely to be of relevance to studying flow past bodies at hypersonic velocities.

References

- [1] Sutton G. W., Sherman A., 1965, *Engineering Magnetohydrodynamics*, McGraw Hill, New York
- [2] Bittencourt J.A., 2004, *Fundamentals of Plasma Physics*, Springer - Verlag, New York
- [3] Shang J.S., 2001, *Recent Research in Magneto-aerodynamics*", *Progress in Aerospace Sciences*, **Vol. 37**, pp. 1 - 20
- [4] Brio M., Wu C.C., 1988, *An Upwind Differencing Scheme for the Equations of Ideal Magnetohydrodynamics*, *Journal of Computational Physics*, **Vol 75**, pp. 400 - 422
- [5] Zachary A.L., Colella P.A., 1992, *A Higher-Order Godunov method for the Equations of Ideal Magnetohydrodynamics*, *Journal of Computational Physics*, **Vol 95**, pp. 341 - 347
- [6] Powell K.G., 1994, *A Riemann Solver for Ideal MHD That Works in More Than One Dimension*, ICASE Report 94 - 24
- [7] Powell K.G., Roe P.L., et al, 1999, *A Solution-Adaptive Upwind Scheme for Ideal Magnetohydrodynamics*, *Journal of Computational Physics*, **Vol 154**, pp. 284 - 309
- [8] Li S., 2003, *An HLLC Riemann Solver for Magnetohydrodynamics*, Preprint submitted to Elsevier Science
- [9] Lee D., Deane A., 2004, *A Numerical Implementation of Magnetohydrodynamics using a Staggered Mesh with High Order Godunov Fluxes*, Project Final Report AMSC 663-664, University of Maryland, College Park, Maryland
- [10] Brackbill J.U., Barnes D.C., 1980, *The Effect of Non-Zero $\nabla \cdot \mathbf{B}$ on the Numerical Solution of Magnetohydrodynamic Equations*, *Journal of Computational Physics*, **Vol 35**, pp. 426 - 430
- [11] Myong R.S., Roe P.L., 1998, *On Godunov-type schemes for Magnetohydrodynamics*, *Journal of Computational Physics*, **Vol 147**, pp. 545 - 567
- [12] Cargo P., Gallice G., 1997, *Roe Matrices for Ideal MHD and Systematic Construction of Roe Matrices for Systems of Conservation Laws*, *Journal of Computational Physics*, **Vol 136**, pp. 446 - 466
- [13] Roe P.L., Balsara D.S., 1996, *Notes on the Eigensystem of Magnetohydrodynamics*, *SIAM Journal of Applied Mathematics*, **Vol 56**, No 1, pp. 57 - 67

- [14] Jiang G.S., Shu C.W., 1999, *A High Order WENO Finite Difference Scheme for the Equations of Ideal Magnetohydrodynamics*, Journal of Computational Physics, **Vol 150**, pp. 561 - 594
- [15] Torrilhon M., Balsara D.S., 2004, *High Order WENO schemes: investigations on non-uniform convergence for MHD Riemann problems*, Journal of Computational Physics, **Vol 201**, pp. 586 - 600
- [16] Toth G., 2000, *The $\nabla \cdot \mathbf{B} = 0$ Constraint in Shock Capturing Magnetohydrodynamics Codes*, Journal of Computational Physics, **Vol. 161**, pp. 605 - 652
- [17] Londrillo P., Del Zanna L., 2004, *On the divergence-free condition in Godunov-type schemes for ideal magnetohydrodynamics: the upwind constrained transport method*, Journal of Computational Physics, **Vol. 195**, pp. 17 - 48
- [18] Ghosh D., Chatterjee A., 2005, *Higher - Order Non - Oscillatory Schemes in Ideal Magnetohydrodynamics*, Proceedings of the Eighth Annual CFD symposium of the CFD Division, Aeronautical Society of India

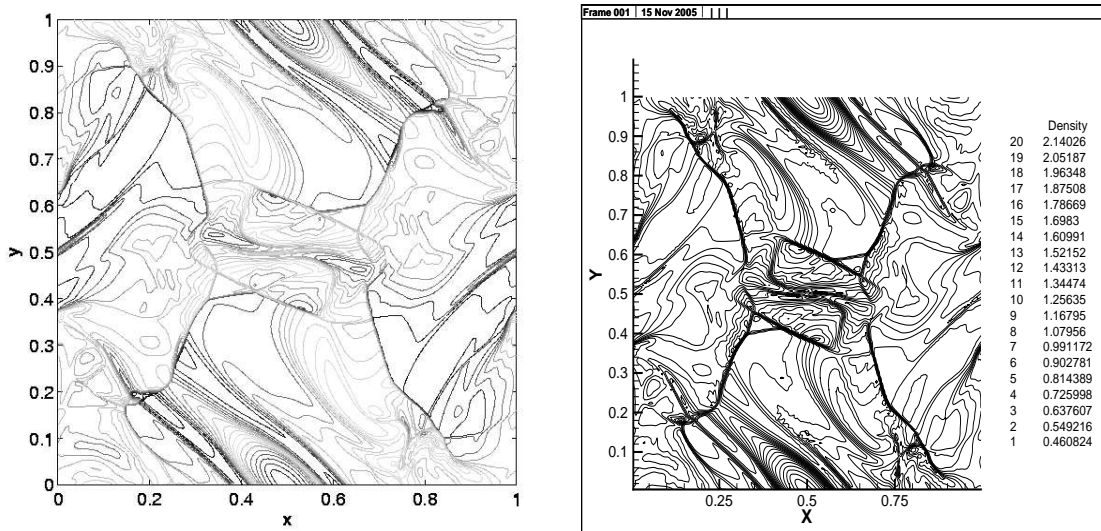


Figure 1: Orszag-Tang Vortex Problem (Density) - Deane & Lee's results [9] and 5th Order WENO

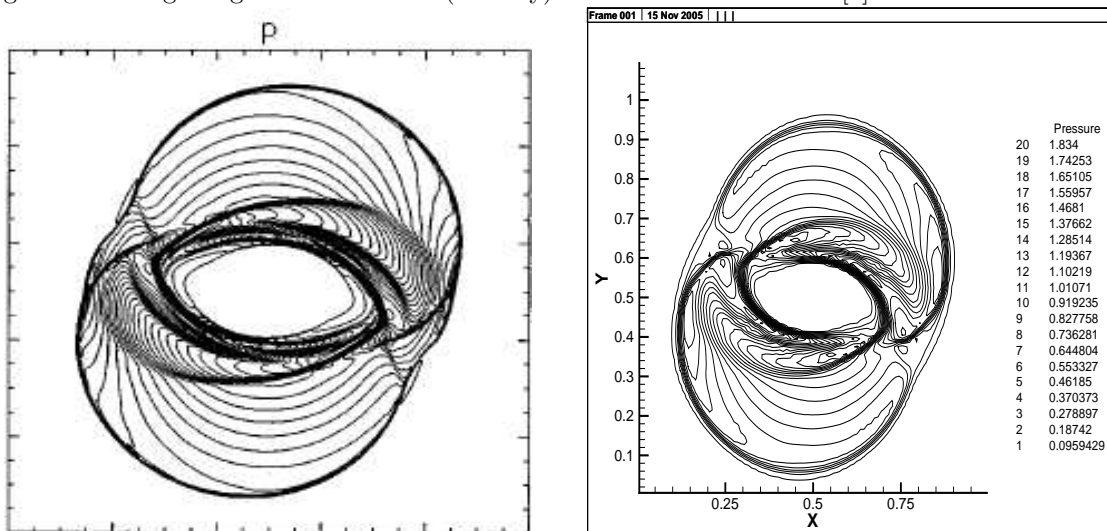


Figure 2: Rotor Problem (Pressure) - Toth's solution [16] and 3rd Order ENO

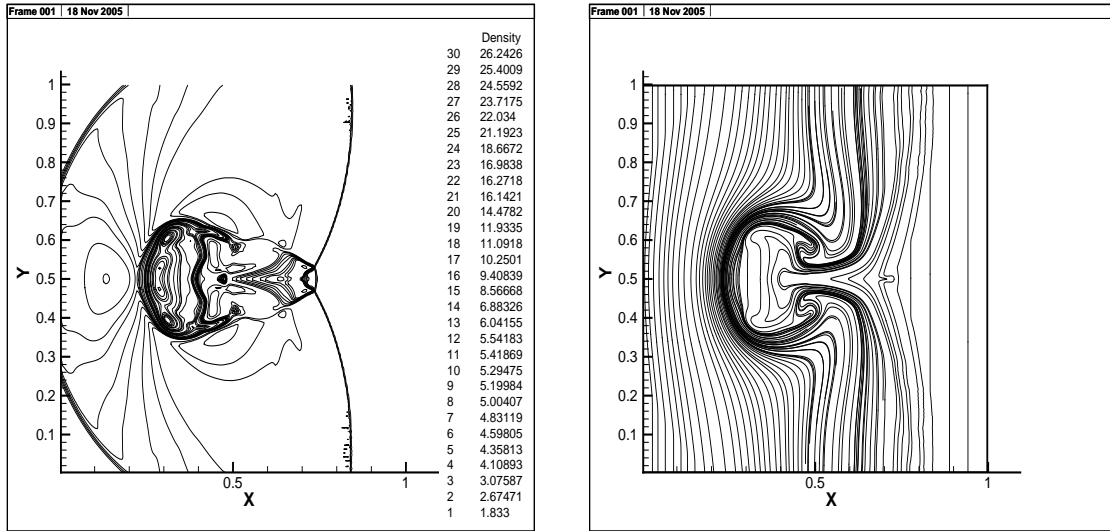


Figure 3: Cloud Shock Interaction (Density and magnetic field line - 2nd order ENO)

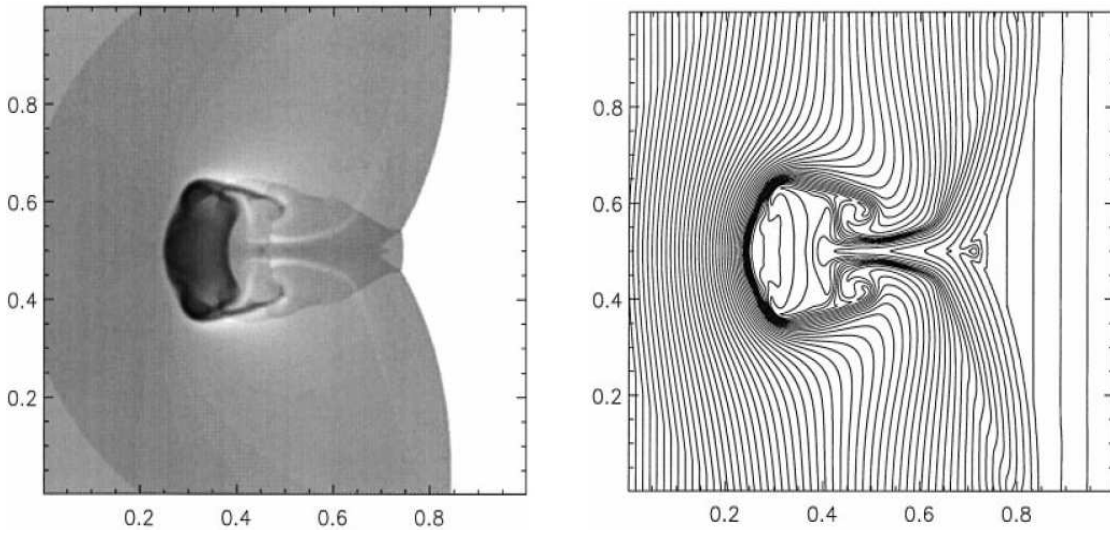


Figure 4: Cloud Shock Interaction (Density and magnetic field lines) - Toth's solution [16]